

Evidence for $B^0 \rightarrow D^+ D^-$ and Observation of $B^- \rightarrow D^0 D^-$ and $B^- \rightarrow D^0 D^{*-}$ Decays

G. Majumder,³⁷ K. Abe,⁶ K. Abe,³⁹ I. Adachi,⁶ H. Aihara,⁴¹ Y. Asano,⁴⁵ V. Aulchenko,¹ T. Aushev,¹⁰ S. Bahinipati,⁴ A. M. Bakich,³⁶ S. Banerjee,³⁷ I. Bedny,¹ U. Bitenc,¹¹ I. Bizjak,¹¹ S. Blyth,²³ A. Bondar,¹ A. Bozek,²⁴ M. Bračko,^{6,17,11} J. Brodzicka,²⁴ T. E. Browder,⁵ M.-C. Chang,²³ P. Chang,²³ Y. Chao,²³ A. Chen,²¹ K.-F. Chen,²³ W. T. Chen,²¹ B. G. Cheon,³ R. Chistov,¹⁰ Y. Choi,³⁵ A. Chuvikov,³¹ S. Cole,³⁶ J. Dalseno,¹⁸ M. Danilov,¹⁰ M. Dash,⁴⁶ A. Drutskoy,⁴ S. Eidelman,¹ Y. Enari,¹⁹ S. Fratina,¹¹ N. Gabyshev,¹ T. Gershon,⁶ A. Go,²¹ G. Gokhroo,³⁷ B. Golob,^{16,11} A. Gorišek,¹¹ J. Haba,⁶ T. Hara,²⁸ N. C. Hastings,⁶ K. Hayasaka,¹⁹ H. Hayashii,²⁰ M. Hazumi,⁶ L. Hinz,¹⁵ T. Hokuue,¹⁹ Y. Hoshi,³⁹ S. Hou,²¹ W.-S. Hou,²³ Y. B. Hsiung,²³ T. Iijima,¹⁹ A. Imoto,²⁰ K. Inami,¹⁹ A. Ishikawa,⁶ R. Itoh,⁶ M. Iwasaki,⁴¹ J. H. Kang,⁴⁷ J. S. Kang,¹³ N. Katayama,⁶ H. Kawai,² T. Kawasaki,²⁶ H. R. Khan,⁴² H. Kichimi,⁶ H. J. Kim,¹⁴ S. K. Kim,³⁴ S. M. Kim,³⁵ P. Križan,^{16,11} P. Krokovny,¹ R. Kulasiri,⁴ S. Kumar,²⁹ C. C. Kuo,²¹ A. Kuzmin,¹ Y.-J. Kwon,⁴⁷ G. Leder,⁹ S. E. Lee,³⁴ T. Lesiak,²⁴ J. Li,³³ S.-W. Lin,²³ D. Liventsev,¹⁰ J. MacNaughton,⁹ F. Mandl,⁹ T. Matsumoto,⁴³ A. Matyja,²⁴ Y. Mikami,⁴⁰ W. Mitaroff,⁹ K. Miyabayashi,²⁰ H. Miyake,²⁸ H. Miyata,²⁶ R. Mizuk,¹⁰ D. Mohapatra,⁴⁶ G. R. Moloney,¹⁸ T. Nagamine,⁴⁰ Y. Nagasaka,⁷ I. Nakamura,⁶ E. Nakano,²⁷ M. Nakao,⁶ H. Nakazawa,⁶ Z. Natkaniec,²⁴ S. Nishida,⁶ O. Nitoh,⁴⁴ S. Ogawa,³⁸ T. Ohshima,¹⁹ T. Okabe,¹⁹ S. Okuno,¹² S. L. Olsen,⁵ W. Ostrowicz,²⁴ H. Ozaki,⁶ H. Palka,²⁴ C. W. Park,³⁵ H. Park,¹⁴ N. Parslow,³⁶ L. S. Peak,³⁶ R. Pestotnik,¹¹ L. E. Piilonen,⁴⁶ M. Rozanska,²⁴ H. Sagawa,⁶ Y. Sakai,⁶ N. Sato,¹⁹ T. Schietinger,¹⁵ O. Schneider,¹⁵ P. Schönmeier,⁴⁰ J. Schümann,²³ M. E. Sevier,¹⁸ H. Shibuya,³⁸ B. Shwartz,¹ V. Sidorov,¹ J. B. Singh,²⁹ A. Somov,⁴ N. Soni,²⁹ R. Stamen,⁶ S. Stanič,^{45,*} M. Starič,¹¹ K. Sumisawa,²⁸ T. Sumiyoshi,⁴³ S. Suzuki,³² S. Y. Suzuki,⁶ O. Tajima,⁶ F. Takasaki,⁶ K. Tamai,⁶ N. Tamura,²⁶ M. Tanaka,⁶ G. N. Taylor,¹⁸ Y. Teramoto,²⁷ X. C. Tian,³⁰ T. Tsukamoto,⁶ S. Uehara,⁶ T. Uglov,¹⁰ K. Ueno,²³ S. Uno,⁶ P. Urquijo,¹⁸ G. Varner,⁵ K. E. Varvell,³⁶ S. Villa,¹⁵ C. C. Wang,²³ C. H. Wang,²² M.-Z. Wang,²³ Y. Watanabe,⁴² Q. L. Xie,⁸ A. Yamaguchi,⁴⁰ Y. Yamashita,²⁵ M. Yamauchi,⁶ Heyoung Yang,³⁴ J. Ying,³⁰ C. C. Zhang,⁸ L. M. Zhang,³³ Z. P. Zhang,³³ V. Zhilich,¹ and D. Žontar^{16,11}

(Belle Collaboration)

¹*Budker Institute of Nuclear Physics, Novosibirsk*²*Chiba University, Chiba*³*Chonnam National University, Kwangju*⁴*University of Cincinnati, Cincinnati, Ohio 45221*⁵*University of Hawaii, Honolulu, Hawaii 96822*⁶*High Energy Accelerator Research Organization (KEK), Tsukuba*⁷*Hiroshima Institute of Technology, Hiroshima*⁸*Institute of High Energy Physics, Chinese Academy of Sciences, Beijing*⁹*Institute of High Energy Physics, Vienna*¹⁰*Institute for Theoretical and Experimental Physics, Moscow*¹¹*J. Stefan Institute, Ljubljana*¹²*Kanagawa University, Yokohama*¹³*Korea University, Seoul*¹⁴*Kyungpook National University, Taegu*¹⁵*Swiss Federal Institute of Technology of Lausanne, EPFL, Lausanne*¹⁶*University of Ljubljana, Ljubljana*¹⁷*University of Maribor, Maribor*¹⁸*University of Melbourne, Victoria*¹⁹*Nagoya University, Nagoya*²⁰*Nara Women's University, Nara*²¹*National Central University, Chung-li*²²*National United University, Miao Li*²³*Department of Physics, National Taiwan University, Taipei*²⁴*H. Niewodniczanski Institute of Nuclear Physics, Krakow*²⁵*Nihon Dental College, Niigata*²⁶*Niigata University, Niigata*²⁷*Osaka City University, Osaka*²⁸*Osaka University, Osaka*²⁹*Panjab University, Chandigarh*³⁰*Peking University, Beijing*

³¹Princeton University, Princeton, New Jersey 08544³²Saga University, Saga³³University of Science and Technology of China, Hefei³⁴Seoul National University, Seoul³⁵Sungkyunkwan University, Suwon³⁶University of Sydney, Sydney NSW³⁷Tata Institute of Fundamental Research, Bombay³⁸Toho University, Funabashi³⁹Tohoku Gakuin University, Tagajo⁴⁰Tohoku University, Sendai⁴¹Department of Physics, University of Tokyo, Tokyo⁴²Tokyo Institute of Technology, Tokyo⁴³Tokyo Metropolitan University, Tokyo⁴⁴Tokyo University of Agriculture and Technology, Tokyo⁴⁵University of Tsukuba, Tsukuba⁴⁶Virginia Polytechnic Institute and State University, Blacksburg, Virginia 24061⁴⁷Yonsei University, Seoul

(Received 20 February 2005; published 20 July 2005)

We report evidence for $B^0 \rightarrow D^+D^-$ and the first observation of the decay modes $B^- \rightarrow D^0D^-$ and $B^- \rightarrow D^0D^{*-}$ based on a sample of $152 \times 10^6 B\bar{B}$ events collected by the Belle detector at KEKB. The branching fractions for $B^0 \rightarrow D^+D^-$, $B^- \rightarrow D^0D^-$, and $B^- \rightarrow D^0D^{*-}$ are found to be $(1.91 \pm 0.51 \pm 0.30) \times 10^{-4}$, $(4.83 \pm 0.78 \pm 0.58) \times 10^{-4}$, and $(4.57 \pm 0.71 \pm 0.56) \times 10^{-4}$, respectively. Charge asymmetries in the $B^- \rightarrow D^0D^-$ and $B^- \rightarrow D^0D^{*-}$ channels are consistent with zero.

DOI: 10.1103/PhysRevLett.95.041803

PACS numbers: 13.25.Hw, 11.30.Er

Mixing induced CP -violating asymmetries in $b \rightarrow c\bar{c}s$ decays have been observed at the B factory experiments, Belle, and BABAR, at levels consistent with standard model (SM) predictions [1]. Cabibbo-suppressed double charm decays (e.g., $B^0 \rightarrow D^{(*)+}D^{(*)-}$) are dominated by $b \rightarrow c\bar{c}d$ tree diagram contributions. Additional penguin contributions with a different weak phase are expected to be small in comparison with tree diagram contributions. Hence, time dependent CP -violating asymmetries in such double charm decays should be nearly equal to those in $B^0 \rightarrow J/\psi K_S$ ($b \rightarrow c\bar{c}s$) type decays. However, a variety of processes beyond the SM can provide additional sources of CP violation [2]. Thus, the $B^0 \rightarrow D^{(*)+}D^{(*)-}$ decay modes can be used to confirm the SM predictions of CP violation [3] or to look for physics beyond the standard model.

BABAR observed the first Cabibbo suppressed double charm decay, $B^0 \rightarrow D^{*+}D^{*-}$ mode [4]. Subsequently, Belle observed the decay modes $B^0 \rightarrow D^{*+}D^-$ and $B^0 \rightarrow D^+D^{*-}$ [5]. Measurements of time dependent CP -violating asymmetry parameters are also available for these modes [4,6].

While the branching fraction for $B^0 \rightarrow D^+D^-$ is expected to be fairly large, evidence for this decay mode has not yet been reported. Using SU(3) symmetry and the world-average branching fraction [7], $\mathcal{B}(B^0 \rightarrow D^+D^-)$ is estimated to be $\sin^2\theta_c \times \mathcal{B}(B^0 \rightarrow D_s^+D^-) \simeq (4.0 \pm 1.5) \times 10^{-4}$, where θ_c is the Cabibbo angle.

The decay modes $B^- \rightarrow D^0D^-$ and $B^- \rightarrow D^0D^{*-}$ are expected to be dominated by tree diagrams with some additional contributions from penguin diagrams. Scaling from the well-measured branching fractions for the Cabibbo-favored processes $B^- \rightarrow D^0D_s^-$ and $B^- \rightarrow D^0D_s^{*-}/B^- \rightarrow D^{*0}D_s^-$, one can estimate the branching fractions of

these two decay modes to be $(6.5 \pm 2.0) \times 10^{-4}$ and $(5.1 \pm 2.2) \times 10^{-4}$, respectively. Assuming SU(3) symmetry, measurement of these branching fractions will enable better understanding of penguin processes.

Here, we report evidence for the decay $B^0 \rightarrow D^+D^-$ and the first observation of the decays $B^- \rightarrow D^0D^-$ and $B^- \rightarrow D^0D^{*-}$. Inclusion of charge conjugate modes is implied throughout this Letter. The analysis is based on a 140 fb^{-1} data sample at the $\Upsilon(4S)$ resonance (10.58 GeV) and a 16 fb^{-1} data sample 60 MeV below the $\Upsilon(4S)$ peak (referred to as off-resonance data), collected with the Belle detector [8] at the energy asymmetric e^+e^- collider KEKB [9]. The data sample contains $152 \times 10^6 B\bar{B}$ events. The fractions of neutral and charged B mesons produced at the $\Upsilon(4S)$ peak are assumed to be equal.

The Belle detector is a general purpose magnetic spectrometer with a 1.5 T magnetic field provided by a superconducting solenoid. Charged particles are measured using a 50 layer central drift chamber (CDC) and a three layer double sided silicon vertex detector (SVD). Photons are detected in an electromagnetic calorimeter (ECL) consisting of 8736 CsI(Tl) crystals. Exploiting the information acquired from an array of 128 time-of-flight counters (TOF), an array of 1188 silica aerogel Čerenkov threshold counters (ACC), and dE/dx measurements in the CDC, we derive particle identification (PID) likelihoods $\mathcal{L}_{\pi/K}$. A kaon candidate is identified by a requirement on the likelihood ratio $\mathcal{L}_K/(\mathcal{L}_K + \mathcal{L}_\pi)$ such that the average kaon identification efficiency is $\sim 93\%$ with pion misidentification rate of $\sim 10\%$. Similarly, charged pions are selected with an efficiency of $\sim 95\%$ and kaon misidentification rate of $\sim 10\%$. We select charged pions and kaons that originate from the region $dr < 1 \text{ cm}$ and $|dz| < 4 \text{ cm}$ with respect to

the run dependent interaction points (IP), where dr , dz are the distances of closest approach of π/K tracks to the IP in the plane perpendicular to and along the z axis (the z axis is defined as passing through the nominal interaction point and antiparallel to the positron beam). All tracks compatible with the electron hypothesis ($\sim 0.2\%$ misidentification rates from a pion or kaon) are eliminated. No attempt has been made to identify muons, which represent a background of about 2.7% to the pion tracks.

Neutral kaons (K_S) are reconstructed via the decay $K_S \rightarrow \pi^+ \pi^-$ with no particle identification requirement for daughter pions. The two-pion invariant mass is required to be within 11 MeV/ c^2 ($\sim 3.5\sigma$, where σ is the invariant mass resolution of $\pi^+ \pi^-$) of the K_S mass. To improve the purity of K_S candidates, we impose K_S momentum-dependent criteria on the impact parameter of the pions, the distance between the closest approaches of the pions along the beam direction, the distance of the $\pi^+ \pi^-$ vertex from the interaction point, and the azimuthal angle difference between the direction of $\pi^+ \pi^-$ vertex from the IP and the K_S momentum direction. Mass and vertex constrained fits are applied to obtain the 4-momenta of K_S candidates. Neutral pions (π^0) are reconstructed from pairs of isolated ECL clusters (photons) with invariant mass in the window $118 \text{ MeV}/c^2 < M_{\gamma\gamma} < 150 \text{ MeV}/c^2$ ($\sim \pm 3\sigma$). The energy of each photon is required to be greater than 30 MeV in the barrel region, defined as $32^\circ < \theta_\gamma < 128^\circ$, and greater than 50 MeV in the end cap regions, defined as $17^\circ < \theta_\gamma \leq 32^\circ$ or $128^\circ < \theta_\gamma \leq 150^\circ$, where θ_γ denotes the polar angle of the photon. Mass constrained fits are applied to obtain the 4-momenta of π^0 candidates.

Beam gas events are rejected using the requirements $|P_z| < 2 \text{ GeV}/c$ and $0.5 < E_{\text{vis}}/\sqrt{s} < 1.25$, in the $Y(4S)$ rest frame, where P_z and E_{vis} are the sum of the longitudinal momentum and the energy of all reconstructed particles, respectively, and \sqrt{s} is the sum of the beam energies in the $Y(4S)$ rest frame. Continuum ($e^+ e^- \rightarrow q\bar{q}$, where $q = u, d, s, c$) events are suppressed by requirements on the ratio of the second to the zeroth Fox-Wolfram moments [10], $R_2 < 0.35$.

The D^0 meson is reconstructed through its decay to $K^- \pi^+$, $K^- \pi^+ \pi^+ \pi^-$, $K_S(\rightarrow \pi^+ \pi^-) \pi^+ \pi^-$, and $K^+ K^-$. The D^+ meson is reconstructed through its decay to $K^- \pi^+ \pi^+$. Mass and vertex constrained fits are applied to improve the D meson momentum resolution.

The tracks from D meson candidates are selected with the criterion, $|dz_i - dz_j| < 2 \text{ cm}$, where $dz_{i(j)}$ is the distance of closest approach of track $i(j)$ to the IP along the z axis. Large combinatorial backgrounds are removed by requiring that the invariant mass of daughter particles is within 2.5σ from the nominal D mass, where σ ($\sim 4.5 \text{ MeV}/c^2$), the mass resolution, depends on the decay chain.

D^{*+} candidates are reconstructed by combining the D^0 with a slow charged pion with $dr < 2 \text{ cm}$ and $|dz| <$

10 cm with respect to the D vertex. D^0 mass windows are widened to $\pm 20 \text{ MeV}/c^2$ for the reconstruction of D^{*+} candidates. D^{*+} candidates are required to have a reconstructed mass difference between the D^{*+} and D^0 within $2.0 \text{ MeV}/c^2$ ($\sim 3.0\sigma$) of the nominal mass difference. A kinematic fit with the D^{*+} mass is applied to obtain the 4-momenta of the D^{*+} candidate.

To reduce large combinatorial backgrounds in D^0 decays to $K^- \pi^+ \pi^+ \pi^-$, a tighter impact parameter requirement, $dr < 0.5 \text{ cm}$, is applied to all four tracks. Note that this requirement is not applied for $D^{*+} \rightarrow D^0(\rightarrow K^- \pi^+ \pi^+ \pi^-) \pi^+$ candidates because this mode has much less background. Similarly, the $D^0 \rightarrow K^- \pi^+ \pi^0$ subdecay mode is included in the reconstruction of D^{*+} candidates due to better signal to background ratio in this decay mode.

Combinations of $D\bar{D}^{(*)}$ are used to reconstruct candidate B mesons. $D\bar{D}^{(*)}$ signals are contaminated with background from misidentified D mesons as well as combinations of two D candidates from opposite B mesons. There are two important kinematic variables used to extract signals from these backgrounds: (i) the energy difference, ΔE , between the measured energy of the candidate event and the beam energy, E_{beam} , in the $Y(4S)$ rest frame and (ii) the beam energy constrained mass, $M_{\text{bc}} = \sqrt{E_{\text{beam}}^2 - (\sum_i \vec{P}_i)^2}$, where \vec{P}_i are momentum vectors of the primary $D^{(*)}$ candidates in the $Y(4S)$ rest frame. The ΔE distribution is used to extract the signal yield since peaking backgrounds are expected in the M_{bc} distributions. The fit is performed for events where M_{bc} satisfies $5.272 \text{ GeV}/c^2 < M_{\text{bc}} < 5.288 \text{ GeV}/c^2$ and the fit range in ΔE is from -70 MeV to 200 MeV . The restricted range in negative ΔE is chosen to exclude contributions from other B decays, such as $B^0 \rightarrow \bar{D}^0 D^{*0}(D^{*0} \rightarrow D^0 \gamma)$. The selected events contain multiple B candidates with a multiplicity depending on the signal channels, which varies from 1.02 to 1.07. In events with more than one candidate B meson, the candidate with the smallest $\chi^2 (= (\Delta M_{D_1}/\sigma_{M_{D_1}})^2 + (\Delta M_{D_2}/\sigma_{M_{D_2}})^2)$ is chosen, where ΔM_{D_i} is the difference of the reconstructed and nominal mass of D_i , and $\sigma_{M_{D_i}}$ is the resolution in M_{D_i} . In $B^- \rightarrow D^0 D^{*-}$ candidates, a $(\Delta M_{D^{*-}}/\sigma_{M_{D^{*-}}})^2$ term is also added to the χ^2 to choose the best candidate, where $\Delta M_{D^{*-}}$ is the difference between measured and nominal mass difference between D^{*-} and \bar{D}^0 , and $\sigma_{M_{D^{*-}}}$ is the resolution in measured mass difference.

Unbinned extended maximum likelihood fits to ΔE distributions are used to extract the signal yields. The signal shape is modeled as a sum of two Gaussians,

$$F(\Delta E) = A \left[\exp \left[-0.5 \left(\frac{\Delta E - \mu}{\sigma} \right)^2 \right] + f_1 \exp \left[-0.5 \left(\frac{\Delta E - \mu}{f_2 \sigma} \right)^2 \right] \right], \quad (1)$$

which is dominated by a Gaussian of width, $\sigma \sim 6 \text{ MeV}$

and a wider Gaussian, whose width is ~ 2 – 3 times larger than the main Gaussian function, but whose contribution is only 15%–17% of the main Gaussian function. Backgrounds are modeled with a linear function.

A signal Monte Carlo (MC) calculation is fitted with this function to determine f_1 and f_2 . The fitted values of f_1 and f_2 are 0.051 and 2.48, respectively. The ΔE distribution in data is wider than in MC calculations. The decay channel, $B^- \rightarrow D^0 D_s^-$, is used as a control sample to calculate the scaling factor, $f (= [\sigma_{\text{data}}/\sigma_{\text{MC}}]_{B^- \rightarrow D^0 D_s^-} = 1.08 \pm 0.05)$ of the Gaussian width in data.

To extract signal yields from data, the width of the main Gaussian function is fixed to $\sigma = f\sigma_{\text{MC}}$ and the remaining four parameters (parameters A and μ of signal function and two parameters of the linear background function) are determined in the fit.

Signal and backgrounds are studied with Monte Carlo event samples that are generated using the QQ event generator [11]. The response of the Belle detector is simulated by a GEANT3-based program [12]. The simulated events are reconstructed and analyzed with the same procedure as is used for the real data. A large generic $B\bar{B}$ MC calculation sample, with a luminosity equivalent to 330 fb^{-1} of data, is used to search for peaking backgrounds in the ΔE distributions. We have also studied feed-across among these signals and from other $B \rightarrow \bar{D}^{(*)}\bar{D}^{(*)}$ decays. Background due to continuum events are studied by analyzing the 16 fb^{-1} of off-resonance data and simulated MC calculation events equivalent to $\sim 330 \text{ fb}^{-1}$ of data. Another large sample of generic $B\bar{B}$ MC calculation sample, equivalent to $\sim 204 \text{ fb}^{-1}$, is also generated using the EVTGEN [13] event generator. No peaking backgrounds are observed in the ΔE distributions of any of these samples.

Signal efficiencies, averaged over the reconstructed sub-decay modes in $B^0 \rightarrow D^+ D^-$, $B^- \rightarrow D^0 D^-$, and $B^- \rightarrow D^0 D^{*-}$ signals are $11.42 \pm 0.10\%$, $10.52 \pm 0.14\%$, and $4.28 \pm 0.08\%$, respectively. Candidate \bar{K}^0 mesons are reconstructed in the $\pi^+ \pi^-$ mode for $D^0 \rightarrow \bar{K}^0 \rightarrow \pi^+ \pi^-$ candidates; thus the \bar{K}^0 to $\pi^+ \pi^-$ branching fraction is included in the average signal efficiencies.

Figure 1 shows the ΔE distributions in data for the decay modes $B^0 \rightarrow D^+ D^-$, $B^- \rightarrow D^0 D^-$, and $B^- \rightarrow D^0 D^{*-}$. There are clear enhancements near $\Delta E = 0$. The corresponding ΔE distributions for events in the M_{bc} sideband region ($5.2 \text{ GeV}/c^2 < M_{\text{bc}} < 5.26 \text{ GeV}/c^2$) do not show any structure. To check for possible background from modes such as $B \rightarrow DK\pi$, $B \rightarrow DK\pi\pi$ or charmless $B \rightarrow K\pi K(n\pi)$, we also examine the B signal yield for combinations when one of the D candidates has an invariant mass in a sideband outside the nominal D mass window. No such backgrounds are observed.

The results of the fits for these decay modes are shown as curves in Fig. 1. The signal yields obtained from the fits are given in Table I. The statistical significance of the yields, defined as $\sqrt{-2 \ln(\mathcal{L}_0/\mathcal{L}_{\text{max}})}$, where $\mathcal{L}_0(\mathcal{L}_{\text{max}})$ is the

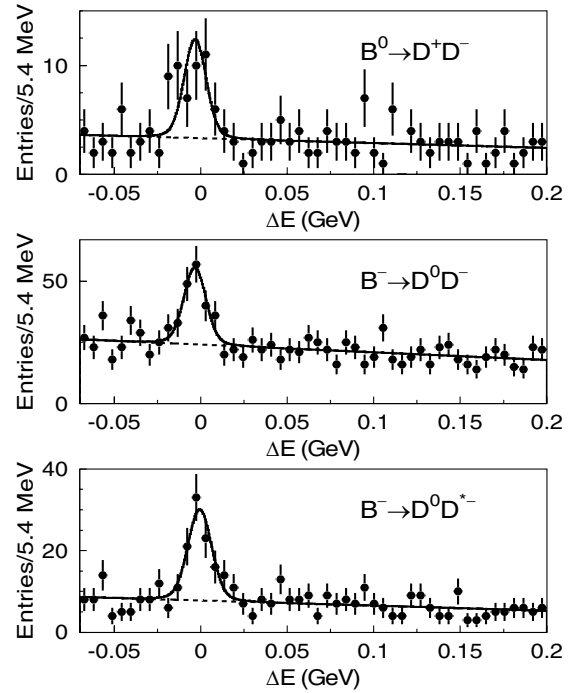


FIG. 1. Fit results of ΔE distributions in data. Points with error bars are the observed events in data, solid lines are the results from the fit, and dashed lines represent the background components.

maximum likelihood without (with) the signal contribution, is also given in that table.

Branching fractions obtained for these three modes are listed in Table I, where the first error is statistical and the second error is systematic. This is the first measurement of the branching fractions for these decay modes. All results are consistent with the expectation from SU(3) symmetry. As a consistency check, the M_{bc} distributions are also fitted after constraining $|\Delta E| < 40 \text{ MeV}$ and show consistent signal yields.

The distribution of the helicity angle for $B^- \rightarrow D^0 D^{*-}$ channel is also studied. The helicity angle, Θ , is defined as the angle between the direction opposite to the B meson and that of the slow pion in the D^{*-} rest frame. Figure 2 shows the ΔE sideband subtracted (the signal region is defined as $|\Delta E| < 20 \text{ MeV}$ and sideband regions are $50 \text{ MeV} < |\Delta E| < 70 \text{ MeV}$) helicity angle distributions in data and for the MC calculation signal. The data follow a $\cos^2\Theta$ distribution as expected for a B to pseudoscalar-vector decay.

TABLE I. Observed signal yields, statistical significances (σ), and branching fractions.

Channel	N_{obs}	σ	$\mathcal{B} \times 10^4$
$B^0 \rightarrow D^+ D^-$	28.0 ± 7.4	4.8	$1.91 \pm 0.51 \pm 0.30$
$B^- \rightarrow D^0 D^-$	92.3 ± 15.8	7.3	$4.83 \pm 0.78 \pm 0.58$
$B^- \rightarrow D^0 D^{*-}$	73.6 ± 11.5	8.2	$4.57 \pm 0.71 \pm 0.56$

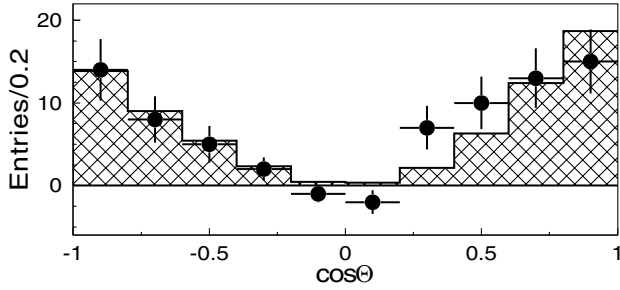


FIG. 2. Background-subtracted distribution of the cosine of the helicity angle in $D^{*-} \rightarrow \bar{D}^0 \pi^-$ decay for $B^- \rightarrow D^0 D^{*-}$ candidates in data (points with error bars) and for $B^- \rightarrow D^0 D^{*-}$ signal MC calculation (hatched histogram).

The systematic uncertainty, shown in Table II, is obtained from a quadratic sum of the uncertainties in (a) the track finding efficiency, ranging from 1% for high momentum tracks to 8% for pions of 80 MeV/c, estimated from partially reconstructed $D^{*-} \rightarrow \bar{D}^0 (\rightarrow K_S (\rightarrow \pi^+ \pi^-) \pi^+ \pi^-) \pi^-$ events and a track embedding study; (b) the π^0 reconstruction efficiency, estimated from a comparison of $D^0 \rightarrow K^- \pi^+ \pi^0$ yields in data and MC calculation; (c) the K_S selection efficiency, estimated from a comparison of $D^0 \rightarrow K_S \pi^+ \pi^-$ yields in data and MC calculation; (d) K/π selection efficiencies, estimated using $D^{*-} \rightarrow \bar{D}^0 (\rightarrow K^+ \pi^-) \pi^-$ events; (e) the world-average D^0 , D^+ , and D^{*+} branching fractions [7]; (f) scaling factor for ΔE distributions in data; (g) MC calculation statistics; (h) the total number of $B\bar{B}$ events ($N_{B\bar{B}}$). The systematic error is also studied by (a) varying the ΔE fit ranges within -200 MeV to $+200$ MeV; (b) the choice of the fitting functions; (c) deriving the branching fraction without selection of the best candidate. Systematic uncertainties from the latter three sources are negligible compared to those from the other sources.

The charge asymmetry, $A = (N_- - N_+)/ (N_- + N_+)$, in $B^- \rightarrow D^0 D^-$ and $B^- \rightarrow D^0 D^{*-}$ channels is $-0.07 \pm 0.16 \pm 0.05$ and $0.15 \pm 0.15 \pm 0.05$, respectively, where

TABLE II. Individual contributions to the systematic uncertainty (in %).

	$D^+ D^-$	$D^0 D^-$	$D^0 D^{*-}$
Track finding	6.4	7.2	9.1
π^0	2.0
K_S	...	0.4	1.0
K/π selection	5.8	5.8	5.1
ΔE scale	2.4	2.6	2.2
MC calculation statistics	0.9	1.3	1.9
$N_{B\bar{B}}$	0.5	0.5	0.5
D branching fractions	13.0	7.0	4.9
Total	15.9	12.0	12.3

$N_-(N_+)$ is the number of observed events in $B^-(B^+)$ decays. Systematic errors on charge asymmetries are determined from high statistics $B^- \rightarrow D^{(*)0} D_s^{(*)-}$ and $B^- \rightarrow D^{*0} (n\pi)$ event samples.

In summary, we report evidence for $B^0 \rightarrow D^+ D^-$ and the first observation of the decays $B^- \rightarrow D^0 D^-$ and $B^- \rightarrow D^0 D^{*-}$ using $152 \times 10^6 B\bar{B}$ events. We measure branching fractions for these three decay modes, which are consistent with the expectation from SU(3) symmetry. Charge asymmetries in the $B^- \rightarrow D^0 D^-$ and $B^- \rightarrow D^0 D^{*-}$ are consistent with zero. The $B^0 \rightarrow D^+ D^-$ channel can be used to perform additional studies of time dependent CP violation in $b \rightarrow c\bar{c}d$ decays.

We thank the KEKB group for the excellent operation of the accelerator, the KEK cryogenics group for the efficient operation of the solenoid, and the KEK computer group and the NII for valuable computing and Super-SINET network support. We acknowledge support from MEXT and JSPS (Japan); ARC and DEST (Australia); NSFC (Contract No. 10175071, China); DST (India); the BK21 program of MOEHRD and the CHEP SRC program of KOSEF (Korea); KBN (Contract No. 2P03B 01324, Poland); MIST (Russia); MESS (Slovenia); Swiss NSF; NSC and MOE (Taiwan); and DOE (USA).

*On leave from Nova Gorica Polytechnic, Nova Gorica.

- [1] K. Abe *et al.* (Belle Collaboration), Phys. Rev. D **66**, 071102(R) (2002); B. Aubert *et al.* (BABAR Collaboration), Phys. Rev. Lett. **89**, 201802 (2002).
- [2] Y. Grossman and M.P. Worah, Phys. Lett. B **395**, 241 (1997).
- [3] A.I. Sanda and Zhi-zhong Xing, Phys. Rev. D **56**, 341 (1997).
- [4] B. Aubert *et al.* (BABAR Collaboration), Phys. Rev. Lett. **89**, 061801 (2002).
- [5] K. Abe *et al.* (Belle Collaboration), Phys. Rev. Lett. **89**, 122001 (2002).
- [6] B. Aubert *et al.* (BABAR Collaboration), Phys. Rev. Lett. **90**, 221801 (2003); T. Aushev *et al.* (Belle Collaboration), Phys. Rev. Lett. **93**, 201802 (2004); H. Miyake *et al.* (Belle Collaboration), Phys. Lett. B (to be published).
- [7] S. Eidelman *et al.* (Particle Data Group), Phys. Lett. B **592**, 1 (2004).
- [8] A. Abashian *et al.* (Belle Collaboration), Nucl. Instrum. Methods Phys. Res., Sect. A **479**, 117 (2002).
- [9] S. Kurokawa and E. Kikutani, Nucl. Instrum. Methods Phys. Res., Sect. A **499**, 1 (2003).
- [10] G.C. Fox and S. Wolfram, Phys. Rev. Lett. **41**, 1581 (1978).
- [11] The QQ B meson decay event generator was developed by the CLEO Collaboration, <http://www.lns.cornell.edu/public/CLEO/soft/QQ>.
- [12] CERN Program Library Long Writeup, W5013, CERN, 1993.
- [13] <http://www.slac.stanford.edu/lange/EvtGen>.